



Supplement of

Understanding aerosol–cloud interactions using a single-column model for a cold-air outbreak case during the ACTIVATE campaign

Shuaiqi Tang et al.

Correspondence to: Shuaiqi Tang (shuaiqi.tang@nju.edu.cn) and Hailong Wang (hailong.wang@pnnl.gov)

The copyright of individual parts of the supplement might differ from the article licence.

S1. Comparison of ERA5 forcing and WRF-CRM forcing in the SCM performance

Figure S1 shows the comparison of large-scale forcing from the ERA5 reanalysis and WRF-CRM simulation over the dropsonde region. Compared to the ERA5 forcing (the left panel), the nested WRF-CRM simulation (the right panel) shows stronger cold advection in MBL and weaker subsidence above MBL. The near-surface temperature and moisture in WRF-CRM are lower than ERA5, yielding higher surface latent (21–68 W/m² higher) and sensible (26–55 W/m² higher) heat fluxes.

We configure E3SM-SCM and WRF-LES with the large-scale forcing and surface fluxes from WRF-CRM over the dropsonde domain (the right panel of Fig. S1) to conduct two simulations, referred to as SCM_CRMforcing and LES_CRMforcing, respectively. Comparing the two simulations with models with ERA5 forcing are shown in Figs. S2-S4. Because of the stronger cold and dry air advection and weaker subsidence, both SCM_CRMforcing and LES_CRMforcing simulations generate a colder, dryer, and deeper boundary layer (Figs. S4a and S4b), especially for LES_CRMforcing in which temperature and moisture are not nudged. The cloud layers in both models are generally thicker than using the ERA5 forcing (Fig. S2a), but detailed features are different between SCM and LES. Compared to the E3SM-SCM, SCM_CRMforcing follows the same trend of cloud top reduction rate (Fig. S3a), with a little time lag. Therefore, the cloud grows higher between 15:00 and 16:00 UTC (Fig. S4f) but has smaller LWC and R_{eff} (Figs. S4g and S4i). For LES, the cloud top height in LES_CRMforcing decreases at a slower rate (Fig. S3a), causing a ~500 m higher cloud top between 15:00 and 16:00 UTC (Fig. S4f). Because of the colder temperature, more cloud hydrometeors are converted to the ice phase (Figs. S2c and S2d), with more precipitation falling to the ground (Figs. S3b). This sensitivity study shows a large impact of the large-scale forcing and surface fluxes on cloud properties in the SCM and LES simulations. A proper combination of large-scale dynamics, sub-grid scale parameterizations, and model configurations is needed to obtain optimal performance in simulating MBL clouds.

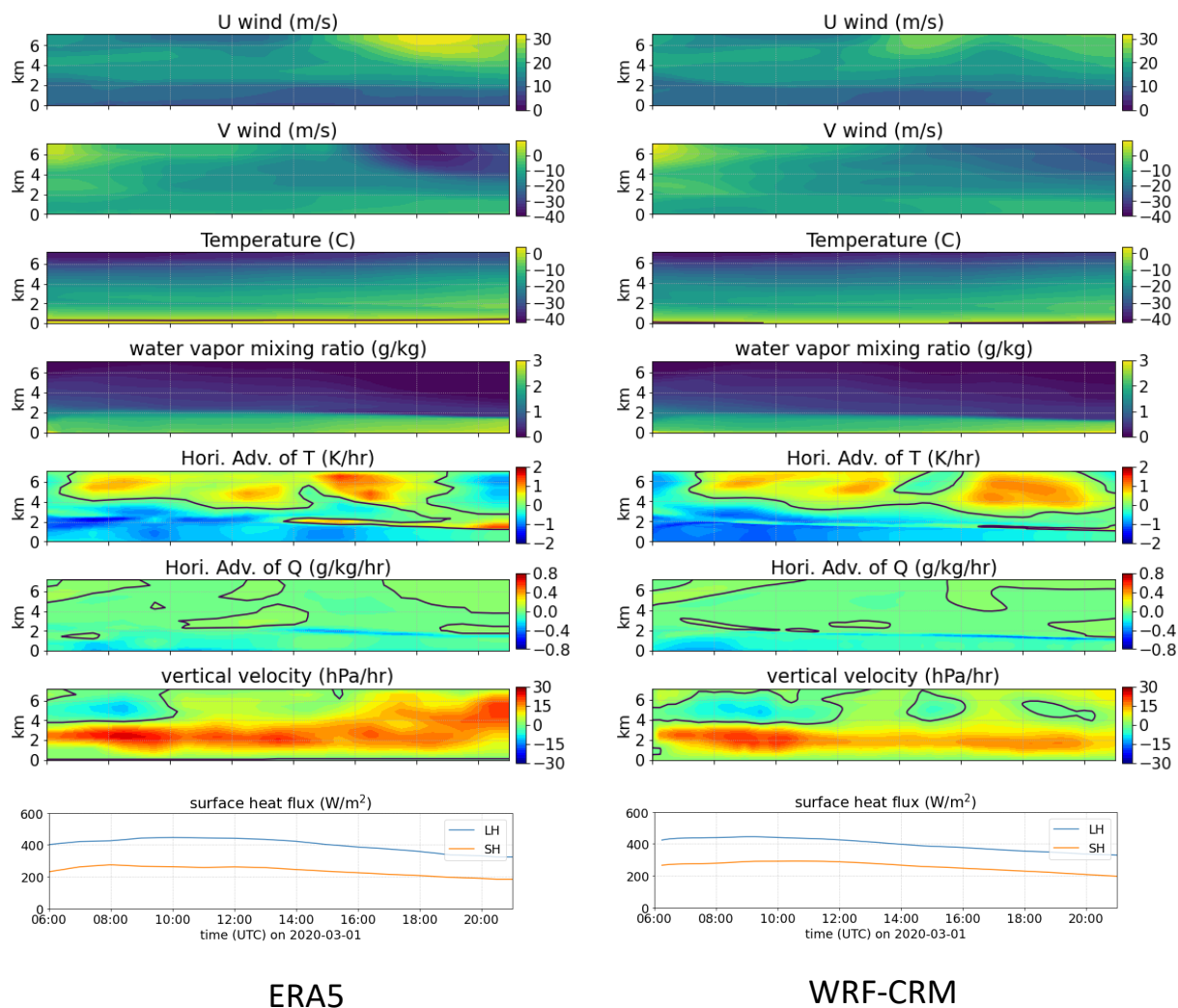


Figure S1: Large-scale environmental conditions, large-scale forcing (horizontal advection and vertical velocity), and surface forcings (latent and sensible heat fluxes) over the dropsonde region from ERA5 used in SCM and WRF-LES (left) and from the WRF-CRM simulations (right). The black lines in large-scale forcing panels mark zero contour.

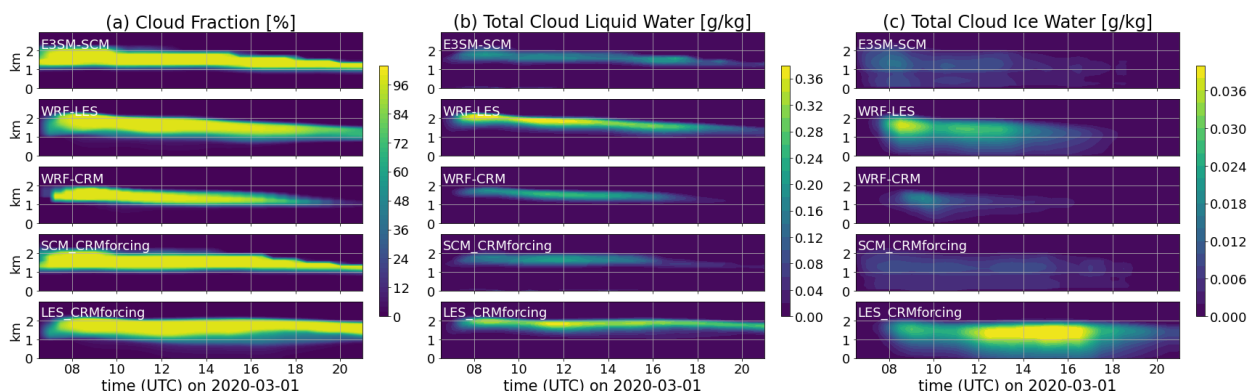


Figure S2: Time-height profiles of cloud fraction, total liquid water, and total ice water produced from different model simulations.

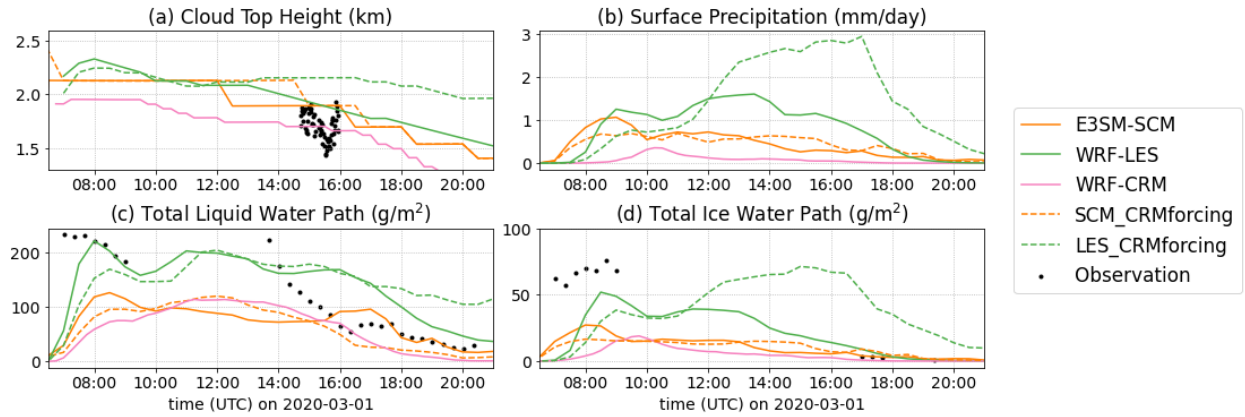


Figure S3: Time series of model simulations (lines) compared with observation (dots) for the 01 March 2020 CAO case. The observation is from aircraft HSRL-2 for cloud top height, GOES-16 retrievals for total liquid (including rain) and total ice (including snow) water paths, for which data points at solar zenith angle greater than 65° are removed.

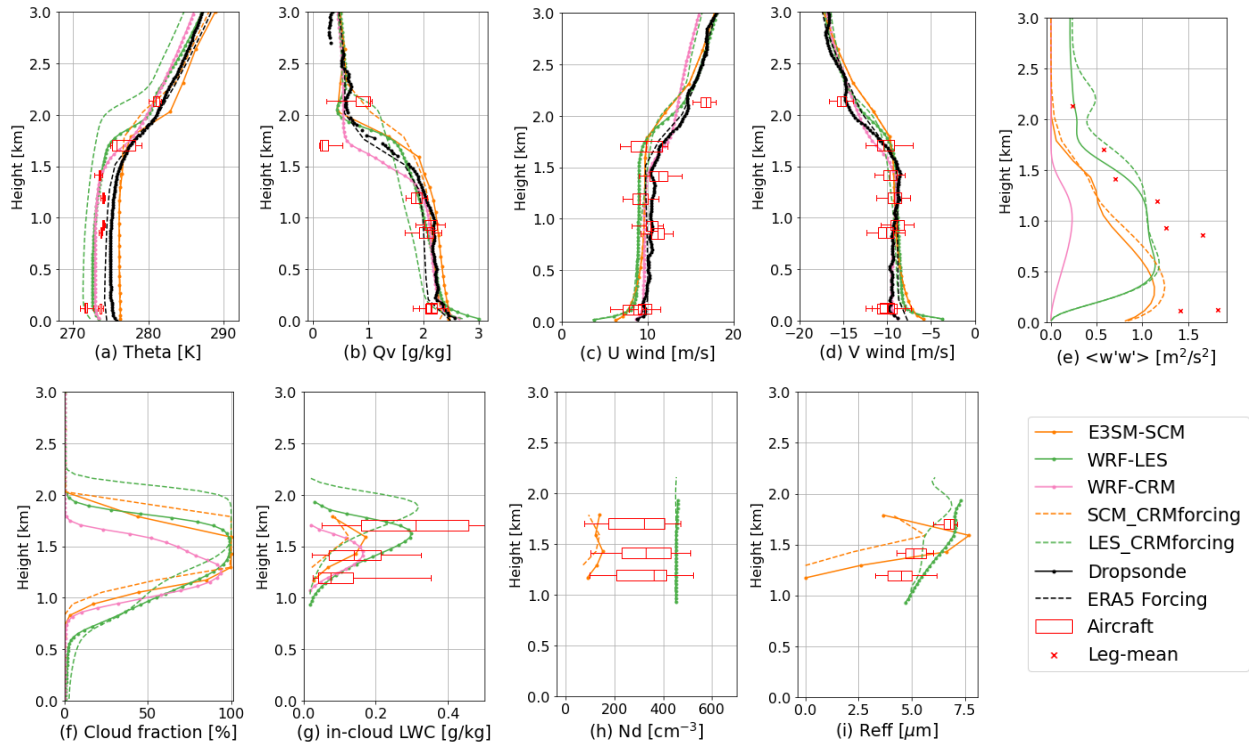


Figure S4: Vertical profiles of atmospheric state, vertical velocity variance, and cloud variables over the analysis domain compared with dropsonde and aircraft measurements. Model profiles are averaged between 15:00 and 16:00 UTC, which is when aircraft measurements were made. The box plots indicate the interquartile ranges of the aircraft

measurements in each flight leg and the whiskers indicate 5th and 95th percentiles, while the red crosses represent vertical velocity variances calculated from 1 Hz measurements in each flight leg. For cloud microphysical variables, a threshold of in-cloud liquid water content $> 0.02 \text{ g/m}^3$ and cloud droplet number $> 20 \text{ cm}^{-3}$ is applied for both model results and aircraft measurements.

S2. Sensitivity to aerosol vertical distribution in SCM

In this set of sensitivity tests, we prescribe aerosols from the BCB2 flight leg only for a single model layer, with all other layers being aerosol-free. We also perform a simulation with idealized aerosol vertical distribution, where aerosol number concentration decreases linearly from 1 km to 2 km AGL (approximately within the cloud layer) to 10% of its boundary-layer value. Figure S6 shows the vertical profiles of the simulation results. With a prescribed aerosol configuration, the cloud activation process only takes the aerosol information in that layer. However, when aerosol particles are activated into cloud droplets, they are redistributed vertically via vertical transport and sedimentation. The aerosols below cloud base and above cloud top do not participate in the cloud activation process, with $N_d = 10 \text{ cm}^{-3}$ (the low cut-off value) and large R_{eff} . Aerosols within the “Cloud Base” and “In-Cloud” layers contribute to about 30% to 40% of N_d activated in the “Constant” aerosol run throughout the simulated cloud layer. The “Cloud Top” aerosols mainly contribute to N_d at the cloud-top layer, with a few droplets falling to lower levels causing a reduction in droplet size (Fig. S5f). The “Idealized” aerosol profile generally captures the vertical distribution of aircraft measured CCN (Fig. S5b), albeit aircraft measured CCN is overall smaller near the cloud base, likely due to the aerosol scavenging process. Although the decrease of aerosols is 90% at the cloud top, the reduction of N_d in the “Idealized” case is only 20% to 30% less than the “Constant” case (Fig. S5e). Since E3SM-SCM underestimates N_d in this case, it is difficult to demonstrate the value of adding aerosol vertical variation. Moreover, the prescribed-aerosol setting in E3SM-SCM limits its ability to study ACI. An interactive aerosol configuration with vertical transport and other processes such as dry and wet deposition enabled is needed to further understand the impact of aerosol vertical distribution on clouds and ACI.

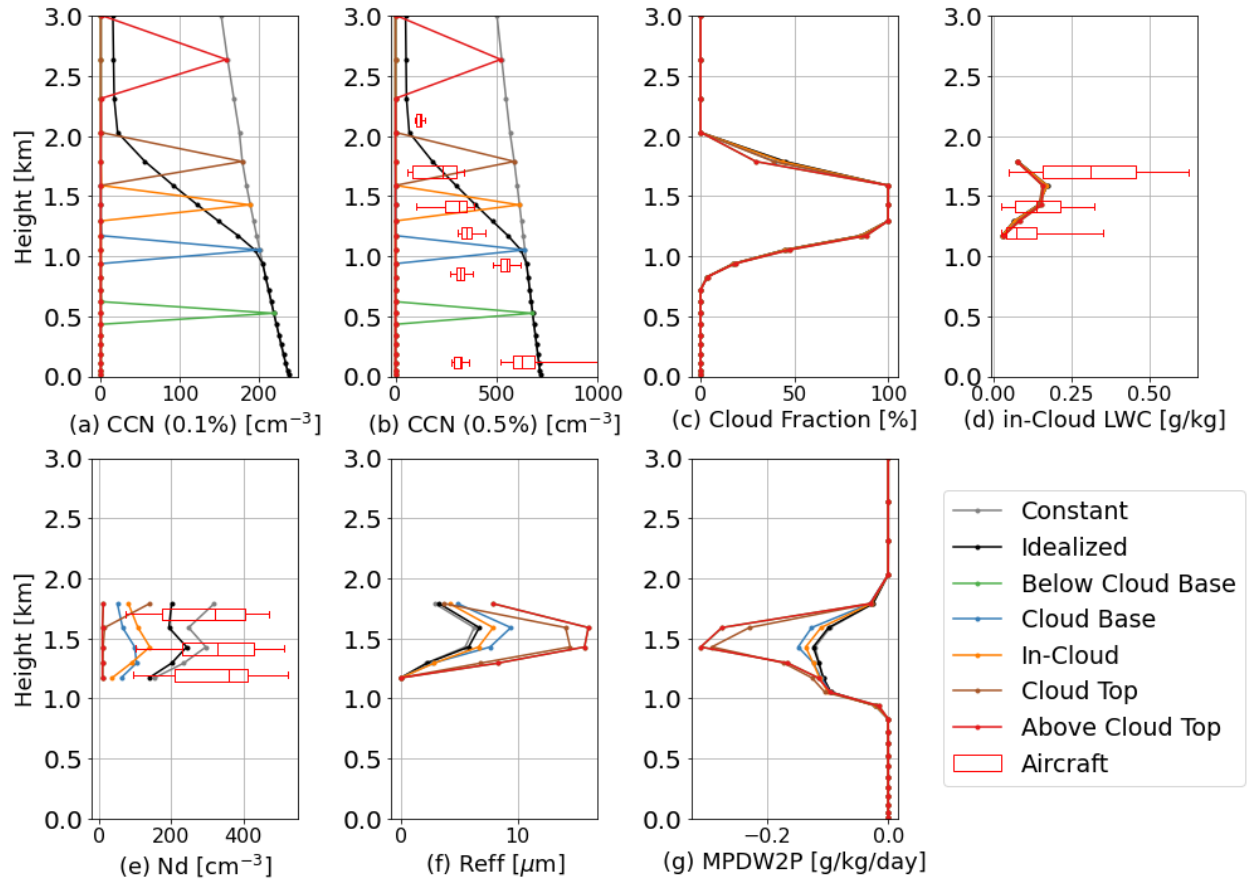


Figure S5: Vertical distributions of (a) CCN number concentrations at 0.1% and (b) 0.5% supersaturation, (c) cloud fraction, (d) in-cloud LWC, (e) N_d , (f) R_{eff} , and (g) cloud water tendency from the conversion-to-precipitation processes in E3SM-SCM simulations with different E3SM-SCM simulations. (Constant): constant aerosol number concentration (per kg air). (Idealized): idealized aerosol profile with number concentration decreases from 1 to 2 km AGL to 10% of the MBL concentration. (Other colour lines): aerosols in a single layer only. Aircraft measured CCN number concentrations for SS between 0.45% and 0.55% are overlaid in (b), and aircraft measured LWC and N_d from the BCB2 leg are overlaid in (d) and (e), respectively. Aerosol composition is from E3SM climatology at the BCB2 leg height.